

Preclinical Properties of ^{18}F -AV-45: A PET Agent for A β Plaques in the Brain

Seok Rye Choi¹, Geoff Golding¹, Zhiping Zhuang¹, Wei Zhang¹, Nathaniel Lim¹, Franz Hefti¹, Tyler E. Benedum¹, Michael R. Kilbourn², Daniel Skovronsky^{1,3}, and Hank F. Kung^{3,4}

¹Avid Radiopharmaceutical Inc., Philadelphia, Pennsylvania; ²Department of Radiology, University of Michigan, Ann Arbor, Michigan; ³Department of Radiology, University of Pennsylvania, Philadelphia, Pennsylvania; and ⁴Department of Pharmacology, University of Pennsylvania, Philadelphia, Pennsylvania

β -amyloid plaques (A β plaques) in the brain, containing predominantly fibrillary A β peptide aggregates, represent a defining pathologic feature of Alzheimer disease (AD). Imaging agents targeting the A β plaques in the living human brain are potentially valuable as biomarkers of pathogenesis processes in AD. (E)-4-(2-(6-(2-(2-(^{18}F -fluoroethoxy)ethoxy)ethoxy)pyridin-3-yl)vinyl)-N-methyl benzenamine (^{18}F -AV-45) is such as an agent currently in phase III clinical studies for PET of A β plaques in the brain. **Methods:** In vitro binding of ^{18}F -AV-45 to A β plaques in the postmortem AD brain tissue was evaluated by in vitro binding assay and autoradiography. In vivo biodistribution of ^{18}F -AV-45 in mice and ex vivo autoradiography of AD transgenic mice (APPswe/PSEN1) with A β aggregates in the brain were performed. Small-animal PET of a monkey brain after an intravenous injection of ^{18}F -AV-45 was evaluated. **Results:** ^{18}F -AV-45 displayed a high binding affinity and specificity to A β plaques (K_d , 3.72 ± 0.30 nM). In vitro autoradiography of postmortem human brain sections showed substantial plaque labeling in AD brains and not in the control brains. Initial high brain uptake and rapid washout from the brain of healthy mice and monkey were observed. Metabolites produced in the blood of healthy mice after an intravenous injection were identified. ^{18}F -AV-45 displayed excellent binding affinity to A β plaques in the AD brain by ex vivo autoradiography in transgenic AD model mice. The results lend support that ^{18}F -AV-45 may be a useful PET agent for detecting A β plaques in the living human brain.

Key Words: PET imaging; Alzheimer disease; β -amyloid plaque; autoradiography; biodistribution

J Nucl Med 2009; 50:1887–1894

DOI: 10.2967/jnumed.109.065284

Alzheimer disease (AD) is a neurodegenerative disease showing an increasingly high incidence in the older population. The presence of β -amyloid plaques (A β plaque) in the brain is a defining pathologic feature for this disease (1,2). Currently, the definitive method to diagnose AD requires the presence of dementia in patients

and, in addition, postmortem histopathology to demonstrate the presence of neuritic plaques, containing predominantly the A β aggregates, and neurofibrillary tangles, predominantly composed of aggregates of τ -protein. PET of A β aggregates in the living human brain may serve as a helpful tool for the diagnosis of AD in living subjects.

Many diverse approaches are being pursued in the quest to obtain a definite diagnosis of AD in living patients. Imaging methods have been used to study structural and functional changes of the brain in the patients with AD, including MRI-based measures of regional brain atrophy. Changes of entorhinal cortex and hippocampal volumes may also be useful for measuring changes in images associated with AD (3). Regional changes in glucose metabolism in the brain, as measured by ^{18}F -FDG PET, can be used to evaluate patients with AD (4,5). However, neither ^{18}F -FDG PET and regional blood flow nor other anatomic imaging studies (MRI) can specifically determine the principal and defining pathologic features of AD, that is, the presence neuritic plaques and neurofibrillary tangles in the brain. A lipophilic tracer, ^{18}F -FDDNP, for binding to both tangles and plaques has been reported (6). Studies in humans suggested that ^{18}F -FDDNP showed a higher retention in regions of brain suspected of having both tangles and plaques (7). The in vivo selectivity of ^{18}F -FDDNP remains to be fully established. Because it binds to both plaques (A β aggregates) and tangles (τ -aggregates) in vitro, it does not selectively recognize a specific pathologic component of AD.

The development of small, neutral, and moderately lipophilic agents targeting A β aggregates in the living human brain was successfully demonstrated using thioflavin T or stilbene as the core structure (8,9). The most commonly known ligands for A β aggregates are listed in Figure 1. Among them, ^{11}C -labeled Pittsburgh compound B (a thioflavin T derivative, PIB), has been most widely studied. PIB showed an excellent initial brain uptake and a high binding affinity to A β plaques (10–12). A wealth of clinical information has been reported using ^{11}C -PIB, and several reports have suggested that there is a correlation of PET images and the presence of A β aggregates in the living

Received Apr. 20, 2009; revision accepted Jul. 22, 2009.

For correspondence or reprints contact: Hank F. Kung, 3700 Market St., Ste 305, Department of Radiology, University of Pennsylvania School of Medicine, Philadelphia, PA 19104.

E-mail: kunghf@gmail.com

COPYRIGHT © 2009 by the Society of Nuclear Medicine, Inc.

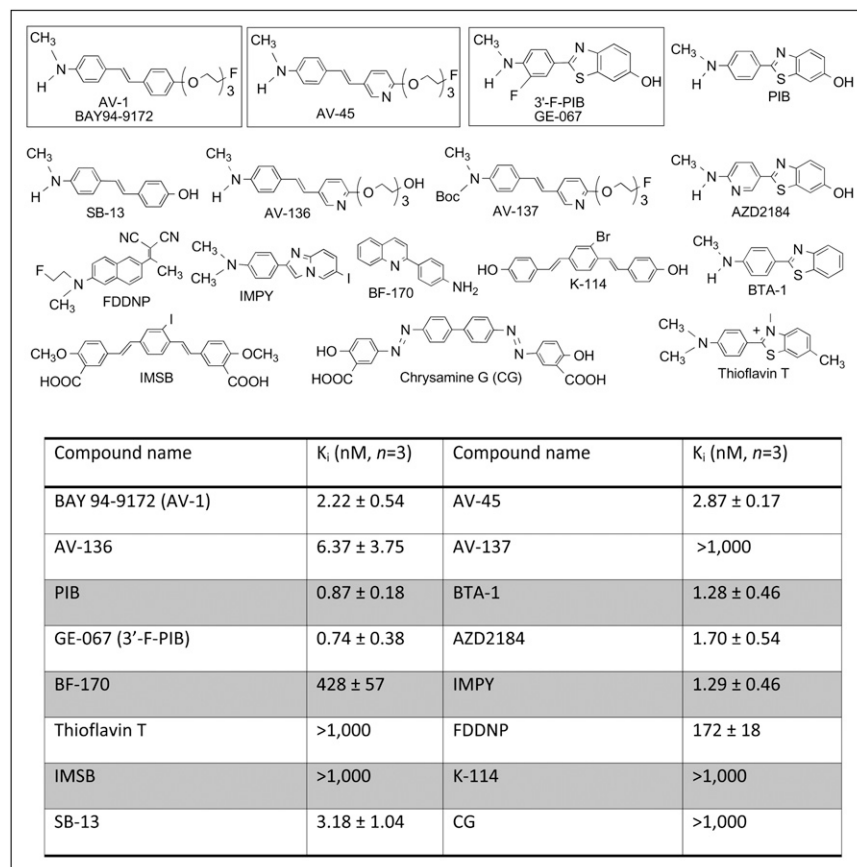


FIGURE 1. Inhibition constants (K_i , nM) of various agents against binding of ^{18}F -AV-45 to $\text{A}\beta$ plaques in postmortem AD brain homogenates.

human brain and postmortem brain tissue samples (13–16). Because ^{11}C has a short physical half-life ($T_{1/2} = 20$ min), a comparable ^{18}F -labeled tracer ($T_{1/2} = 110$ min) will be more useful to expand the applicability of PET in a wider patient population. An ^{18}F -labeled PIB derivative, ^{18}F -3'-F-PIB (GE-067) (Fig. 1), has also been reported (13,17), and it is currently under a phase II clinical trial in Europe, sponsored by GE Healthcare. It was reported recently that ^{123}I -IMPY may be useful as a SPECT agent targeting $\text{A}\beta$ plaques in the brain (18,19). Preliminary clinical data of ^{123}I -IMPY in healthy and AD patients showed a distinct distribution pattern similar to that of ^{11}C -PIB. However, the signal-to-noise ratio for plaque labeling is not robust (20,21). Because of the fast brain and plasma clearance observed in AD and in healthy subjects, the in vivo metabolism and instability of ^{123}I -IMPY may not provide an optimal signal-to-noise ratio. Additional candidates are being explored for SPECT of $\text{A}\beta$ plaques in the brain (22,23).

Previously, stilbene derivatives were identified as ligands that showed a high binding affinity to preformed $\text{A}\beta$ aggregates (24). The rigid structures of stilbene and styrylpyridine have provided core structures for developing many specific imaging agents for $\text{A}\beta$ plaques (25–29). A small and neutral stilbene derivative, ^{11}C -SB-13 (Fig. 1), was prepared and demonstrated an excellent binding affinity. In addition, in vitro autoradiography of ^{11}C -SB-13 displayed excellent labeling of $\text{A}\beta$ plaques densely

populated on postmortem AD brain sections (30). A preliminary human study using ^{11}C -SB-13 for PET showed excellent differential increased uptake and retention in the frontal cortex (in which $\text{A}\beta$ plaques are notably located) of AD patients, as compared with control subjects (31). Despite its success in detecting $\text{A}\beta$ plaques in the living human brain by PET, no further patient studies using ^{11}C -SB-13 were performed. Technical demands associated with producing and performing PET of a ^{11}C tracer limit its widespread clinical application. This situation provided incentives to search for alternative SB-13 derivatives suitably labeled with ^{18}F . Initial attempts on developing ^{18}F -labeled SB-13 by adding a fluoroalkyl substitution group on either end of SB-13 were met with little success. These SB-13 derivatives were too lipophilic and showed high nonspecific binding in the healthy brain. To overcome this problem of too high lipophilicity and to provide a simple ^{18}F labeling procedure, a series of fluoropegylated stilbene derivatives was successfully prepared and tested (26,27,32). There are 2 structurally similar fluoropegylated agents that are currently being developed commercially: BAY 94-9172 (AV-1, in phase II clinical trials by Schering/Bayer) (33) and ^{18}F -AV-45 (AV-45, in phase III clinical trials by Avid Radiopharmaceuticals). Currently, three ^{18}F tracers targeting $\text{A}\beta$ aggregates (BAY 94-9172, GE-067, and AV-45) are in active commercial development.

Reported herein is the preclinical characterization of ^{18}F -AV-45 as an A β plaque imaging agent. In vitro binding studies of ^{18}F -AV-45 with postmortem AD brain tissue homogenates were performed to determine the binding affinity (K_d) and density (B_{max}). Autoradiography of human brain sections using ^{18}F -AV-45 and ex vivo autoradiography of transgenic mice specially engineered to produce excess A β plaques was evaluated to establish the selectivity of the binding to A β plaques. Biodistribution studies in healthy mice (male and female) were performed to measure the brain penetration and kinetics of brain washout. Metabolites of ^{18}F -AV-45 after an intravenous injection into healthy mice were found, and their potential for brain penetration and binding to A β plaque was investigated.

MATERIALS AND METHODS

General

All reagents used for chemical synthesis were commercial products and were used without further purification. Synthesis of precursors and related derivatives was accomplished by previously reported procedures. Two major metabolites (AV-160 and AV-267) were prepared and characterized using schemes similar to those reported for ^{18}F -AV-45 (supplemental information; supplemental materials are available online only at <http://jnm.snmjournals.org>) (29). CD-1 mice (20–26 g, male and female) were used for biodistribution studies. Transgenic mice (APPswePSEN1) were purchased from Jackson Laboratory. All protocols requiring the use of mice were reviewed and approved by the Institutional Animal Care and Use Committee (University of Pennsylvania and University of the Sciences in Philadelphia). Postmortem human samples were obtained from National Disease Research Interchange. Small-animal PET protocols for monkeys were approved by the Institutional Animal Care and Use Committee, University of Michigan.

Radiosynthesis of ^{18}F -AV-45

^{18}F -AV-45 was prepared using a method reported previously (29). Briefly, ^{18}F -fluoride ion trapped on an anion exchange cartridge (purchased from ORTG, Inc.) was eluted to the reaction vessel using 1 mL of aqueous solution consisting of potassium carbonate (50 mg) and Kryptofix (100 mg) in a mixture of H_2O (4 mL) and MeCN (10 mL). The water in the eluted activities was removed by heating to 70°C under a stream of helium and under vacuum, and this process was repeated to yield anhydrous Kryptofix (Sigma Chemicals)/ K_2CO_3 / ^{18}F -fluoride. Approximately 1 mg of *O*-tosylated precursor for making ^{18}F -AV-45 was dissolved in 1 mL of anhydrous dimethyl sulfoxide and added to the reactor mixture containing the anhydrous ^{18}F -fluoride prepared above. The reaction mixture was heated to 120°C for 10 min and then cooled to 50°C before the addition of 0.25 mL of 10% HCl in high-performance liquid chromatography (HPLC)-grade water. The mixture was heated to 120°C for 5 min. After cooling to 50°C, a 0.33-mL portion of 10% NaOH and 5-mL HPLC-grade water were added. The solution was loaded onto a Sep-Pak Light C18 column (Waters) and washed further with 5 mL of HPLC water; the desired ^{18}F -AV-45 was eluted with 1 mL of MeCN into a reservoir containing 2 mL of HPLC solvent (55% MeCN:45% 20 mM aqueous NH_4OAc with 0.5% w/v ascorbic acid sodium salt) and 1 mL of HPLC water. The crude mixture

was then loaded onto a semipreparative HPLC column (Eclipse XDB-C18; Zorbax) (5 μm , 9.4 \times 250 mm; flow rate, 4 mL/min). The HPLC fraction containing the desired ^{18}F -AV-45 was collected into another reservoir containing 15 mL of HPLC water and passed through a preconditioned Sep-Pak Light C-18, which was further washed with 15 mL of sterile water for an injection containing 0.5% w/v ascorbic acid sodium salt. The final product, ^{18}F -AV-45, was eluted with 1 mL of ethanol (United States Pharmacopeia [USP] for injection) into 9 mL of sodium chloride injection (sterile, USP) containing 0.5% w/v ascorbic acid sodium salt (USP). ^{18}F -AV-45 was routinely prepared with a 10%–30% radiochemical yield, a high specific activity (>37,000–185,000 MBq/mmol [$>1,000$ –5,000 Ci/mmol]), and a high radiochemical purity (>99%).

In Vitro Binding Studies of ^{18}F -AV-45

Gray matter of frozen AD brain samples were homogenized with a tissue homogenizer in phosphate-buffered saline (PBS). Tissue homogenates were diluted to 50–100 mg/mL and frozen at -80°C until used for binding assays. Competitive binding assays were performed in 12 \times 75 mm borosilicate glass tubes. The reaction mixture contained 200 μL of AD brain homogenates (20–25 μg), ^{18}F -AV-45 (0.04–0.06 nM diluted in PBS), and 100 μL of competing compounds (10^{-5} to 10^{-10} M diluted serially in PBS containing 0.1% bovine serum albumin) in a final volume of 0.5 mL. Nonspecific binding was defined in the presence of BTA-1 (Fig. 1) (8 μM) in the same assay tubes. The mixture was incubated for 2 h at 37°C, and the bound and the free radioactivity were separated by vacuum filtration through Whatman GF/B filters using a Brandel M-24R cell harvester, followed by washing with PBS buffer 3 times. Filters containing the bound ^{18}F -AV-45 were assayed for radioactivity in a γ -counter (Wizard 3" 1480 automatic γ -counter; Perkin Elmer). Under the assay conditions, the specifically bound fraction was less than 15% of the total radioactivity. The results of inhibition experiments were subjected to nonlinear regression analysis using EBDA (Elsevier-Biosoft) by which inhibition constant (K_i) and K_d values were calculated.

Biodistribution

CD-1 mice (20–26 g, male and female) were injected with ^{18}F -AV-45 (370 kBq [10 μCi], 150 μL formulated in 10% ethanol and 90% saline with 0.5% ascorbic acid) directly into the tail vein. The mice were sacrificed by cardiac puncture under isoflurane anesthesia at various time points (2, 60, 120, and 180 min) after the injection. Organs of interest were removed and weighed, and the radioactivity was counted with a γ -counter. The injected percentage dose per organ was calculated by a comparison of the tissue counts to suitably diluted aliquots of the injected material. Each time point consisted of a group of 3 animals.

Ex Vivo Autoradiography of Transgenic Mouse Brain

Under anesthesia, the transgenic mice (B6.Cg-Tg [APPswePSEN1]; age, 25 mo) were injected with 18,500 kBq (500 μCi) of ^{18}F -AV-45 into the tail vein. For ex vivo autoradiography, a higher dose (500 μCi) was used so that there would be sufficient counts in the brain for exposing the film. The mice were sacrificed at 30 min after tracer injection. Brains were removed and cut into 20- μm sections. The brain sections were exposed to Kodak Biomax MRI film overnight. After the film was developed, the images were digitized.

In Vitro Autoradiography of AD Brain Sections

Frozen brains from AD and control subjects were cut into 20- μ m sections. The sections were incubated with ^{18}F -AV-45 in 40% ethanol at a concentration of 0.3 nM for 1 h. The sections were then dipped in saturated Li_2CO_3 in 40% ethanol (2-min wash twice) and washed with 40% ethanol (2-min wash once), followed by rinsing with water for 30 s. After drying, the sections were exposed to Kodax Biomax MRI film for 12–18 h. After the film was developed, the images were digitized.

Thioflavin S Staining

Brain sections were immersed in 10% neutral buffered formalin for 1 h, and autofluorescence was quenched by treatment with 0.05% KMnO_4 and bleaching in 0.2% $\text{K}_2\text{S}_2\text{O}_5$ /0.2% oxalic acid. Quenched tissue sections were stained with 0.025% thioflavin S in 40% ethanol for 3–5 min. Sections were differentiated in 50% ethanol and viewed using a Nikon E800 fluorescence microscope with a charge-coupled device digital camera.

Metabolite Analysis

Between 370 and 555 MBq (10 and 15 mCi) of ^{18}F -AV-45 were injected into the tail vein of healthy mice. The mice were sacrificed at 2, 10, 30, or 60 min after the injection. The blood samples were centrifuged at 3,000 rpm for 2 min to separate plasma. Plasma samples were mixed with equal volumes of acetonitrile followed by centrifugation at 5,000 rpm for 5 min to remove the denatured proteins. The supernatant was then analyzed directly by HPLC. The HPLC analysis was performed on an Eclipse XDB-C18 column (4.6 \times 150 mm) with 0.1% trifluoroacetic acid water and acetonitrile gradient at a flow rate of 1 mL/min.

For the determination of ^{18}F -AV-45 and its metabolites in the liver and brain, liver and brain were excised and cut into small parts. The tissues were homogenized in 2 mL of PBS and acetonitrile mixture. The homogenates were centrifuged at 5,000 rpm for 3 min. The supernatant was separated from the tissue pellet, the entire supernatant was concentrated under the stream of N_2 gas, and 0.1 mL was analyzed using HPLC in the same way as described for plasma. The retention times under these conditions were approximately 2.2, 4.1, and 7.3 min for polar metabolites; 11.5 min for ^{18}F -AV-160; 12.4 min for ^{18}F -AV-45; and 15.3 min for ^{18}F -AV-267.

Monkey Small-Animal PET

A young adult female rhesus monkey (6.65 kg) was anesthetized (isoflurane) and intubated, a venous catheter was inserted into 1 hindlimb, and the animal was positioned on the bed of the Concorde microPET P4 gantry. Isoflurane anesthesia was continued throughout the study. After completion of the transmission scan, the animal was injected with ^{18}F -AV-45 (173.9 MBq [4.7 mCi]; specific activity, 71,262 MBq/mmol [1,926 Ci/mmol]; in 3 mL of 95% isotonic saline and 5% ethanol) as a bolus over 1 min. Emission data were collected for 90 min (frames, 5 \times 2 min, 10 \times 5 min, and 3 \times 10 min), corrected for attenuation and scatter, and reconstructed using the 3-dimensional maximum a priori method. Regions of interest (ROIs) were drawn manually on multiple planes to obtain volumetric ROIs for the striatum, thalamus, cortex, and white matter, using a summed image of the last 3 frames (60- to 90-min data). The volumetric ROIs were then applied to the full dynamic dataset to obtain the regional tissue time–radioactivity data.

RESULTS

In Vitro Binding Studies of ^{18}F -AV-45 to A β Aggregates in the AD Brain Tissue Homogenates

An in vitro binding assay was used to measure ^{18}F -AV-45 affinity to A β aggregates in the AD brain tissue homogenates. The inhibition constants (K_i , nM) of various agents against binding of ^{18}F -AV-45 to A β aggregates in postmortem AD brain homogenates are presented in Figure 1. ^{18}F -AV-45 displayed excellent binding affinity (2.87 ± 0.17 nM).

To further evaluate the in vitro binding of ^{18}F -AV-45 to A β aggregates in postmortem AD brain homogenates, a series of saturation binding experiments was performed. Results of saturation binding of this ^{18}F tracer in postmortem AD brain homogenates suggested that the binding is specific and saturable. Scatchard analysis suggested that the binding fitted to a single binding site (Fig. 2). Four different AD brain homogenates were tested. The averages of the K_d and B_{max} for these samples were 3.72 ± 0.30 nM and $8,811 \pm 1,643$ fmol/mg protein, respectively.

The kinetics of association and dissociation of ^{18}F -AV-45 with A β aggregates in postmortem AD brain homogenates were also evaluated (Fig. 3). It was determined that the $K_{\text{off}} = 0.045 \pm 0.006 \text{ min}^{-1}$ and the $K_{\text{on}} = 0.034 \text{ min}^{-1}/\text{nM}$; assuming $K_d = K_{\text{off}}/K_{\text{on}}$, then $K_d = 1.31$ nM. Data presented in Figure 3 suggested that the tracer binding to AD brain homogenates was reversible and the K_d derived by this kinetic measurement was comparable to that measured by saturation binding assay.

Autoradiography of Postmortem Brain Tissue Sections with ^{18}F -AV-45

When confirmed healthy and AD brain sections were incubated with ^{18}F -AV-45, the resulting autoradiogram clearly demonstrated a highly dense labeling by this tracer

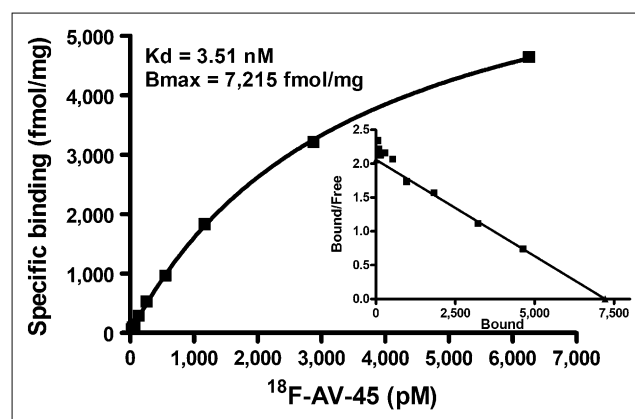


FIGURE 2. Representative saturation binding of ^{18}F -AV-45 to A β plaques in postmortem AD brain homogenates; Scatchard analysis of binding is shown. In this example, K_d was 3.51 nM and B_{max} was 7,215 fmol/mg of protein. Overall, average values for 4 AD cases were $K_d = 3.72 \pm 0.30$ nM and $B_{\text{max}} = 8,811 \pm 1,643$ fmol/mg of protein.

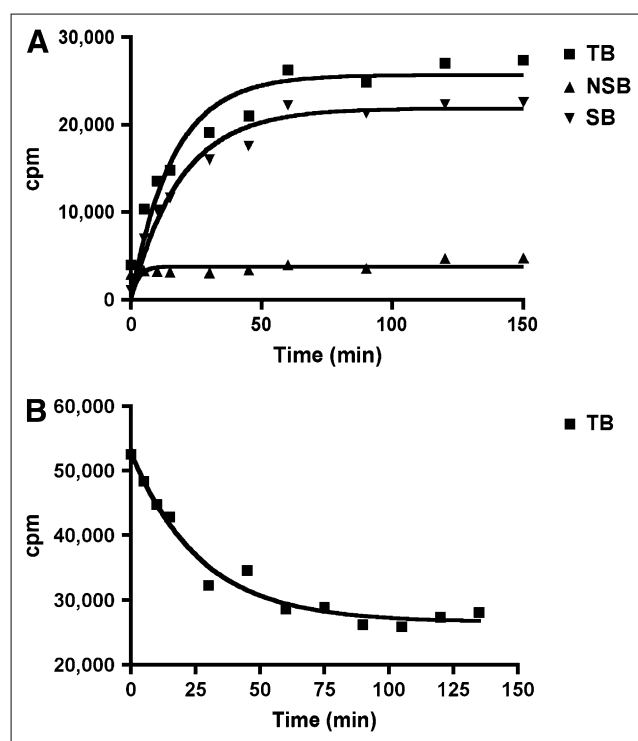


FIGURE 3. Kinetics of association (A) and dissociation (B) of ^{18}F -AV-45 with A β plaques in postmortem AD brain homogenates. TB = total binding; NSB = nonspecific binding; SB = specific binding.

to the AD brain sections containing A β plaques, although there was no specific labeling in the brain sections of control subjects (Fig. 4).

Ex Vivo Autoradiography of Transgenic Mouse Brain

Recent success in the development of transgenic mice specifically engineered to overexpress A β and to generate A β plaques in the brain has provided a convenient animal model of AD for the testing of potential PET agents. ^{18}F -AV-45 was injected intravenously in transgenic mice (APP^{swe}/PSEN1; age, 25 mo), and 30 min after injection the brains were removed, frozen, and sectioned for autoradiography. Autoradiograms of the brain sections showed a dense labeling of the plaques in the cortical regions and hippocampus. The labeling of the plaques was confirmed by costaining with thioflavin S, a dye commonly used for staining the A β plaques in human brain sections. The results was comparable to those reported previously for

BAY 94-9172 (AV-1) and ^{125}I -IMPY in a similar strain of transgenic mice (Fig. 5) (26,34).

In Vivo Biodistribution in Mice

After an intravenous injection in healthy mice, ^{18}F -AV-45 showed desirable biodistribution properties for a brain imaging agent. It entered the brain and reached a peak concentration of 6.23 percentage injected dose per gram (%ID/g) within 2 min after administration and dropped to 1.84 %ID/g within 60 min in female mice and 7.33 %ID/g within 2 min after administration and dropped to 1.88 %ID/g within 60 min in male mice (data included in supplemental information). ^{18}F -AV-45 also distributed to several other organs; the liver and kidneys showed initial uptake with washout, whereas the intestines showed accumulation of radioactivity over time. At 2 min, more than 95% of the total radioactivity injected was accounted for in various organs (biodistribution data in male and female mice are included as supplemental information). The biodistribution data in mice were comparable to those reported previously for ^{11}C -PIB (10) and ^{18}F -BAY 94-9172 (29).

In Vivo Metabolism in Mice

In vivo metabolism of ^{18}F -AV-45 in mice was evaluated after an intravenous injection (Fig. 6). At 30 min after injection, only 30% of the parent, ^{18}F -AV-45, remained in plasma. The biologic $T_{1/2}$ of ^{18}F -AV-45 in mouse plasma was estimated to be less than 30 min. Metabolite profiling and identification of the metabolites were done by HPLC with radioactive detection and liquid chromatography/mass spectroscopy analysis. One of the metabolites in the plasma was the *N*-demethylated ^{18}F -AV-160, which constituted about 48% at 30 min after injection (Fig. 6). The other major radioactive metabolite was identified as the *N*-acetylated derivative ^{18}F -AV-267 (Fig. 6). These 2 metabolites were prepared separately and used for further characterization of their biologic properties such as brain uptake and binding affinity to A β plaques. When injected intravenously at a tracer dose to healthy mice, both metabolites showed good brain uptake, but the uptake was less than that of the parent ^{18}F -AV-45 (Fig. 6). The brain uptake of ^{18}F -AV-160 at 2 min after injection was 4.5 %ID/g of tissue, which at 60 min after injection decreased to 1.8 %ID/g; similarly, the brain uptake of ^{18}F -AV-267 was 3.3 %ID/g at 2 min and 1.8 %ID/g at 60 min after injection. The initial uptake of the parent ^{18}F -AV-45 was 1.5-fold higher than either of its metabolites. No significant binding to A β plaques was observed with either of the metabolites using AD brain-section autoradiography and

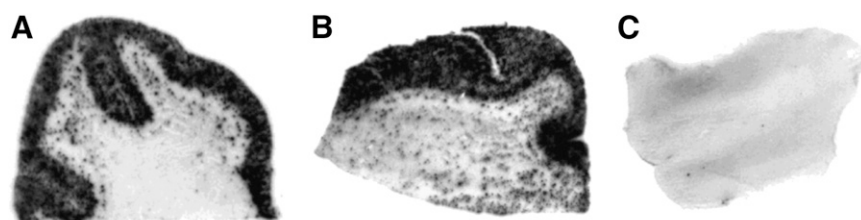


FIGURE 4. In vitro autoradiograms of frozen human brain sections labeled with ^{18}F -AV-45. (A and B) Highly intensive labeling of A β plaques on brain sections from AD patients. (C) Control subject exhibits no labeling by this tracer.

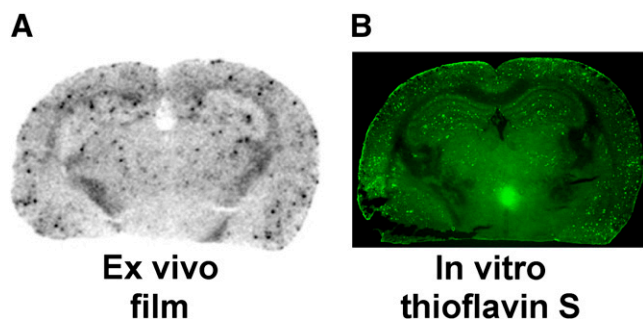


FIGURE 5. Ex vivo autoradiography of ^{18}F -AV-45 in 25-month-old Tg (APPswe/PSEN1) mice. (A) Ex vivo autoradiogram of brain section. (B) Fluorescent image of comparable brain section after thioflavin S staining.

the in vitro AD brain homogenate binding assay described above for ^{18}F -AV-45. The inhibition constants of AV-160 ($K_i = 54 \pm 5$ nM) and AV-267 ($K_i = 398 \pm 45$ nM) indicate at least a 20- to 100-fold reduction of binding affinity to A β plaques in AD brain tissue homogenates, as compared with that of the nonradioactive version of ^{18}F -AV-45 ($K_i = 2.87 \pm 0.17$ nM) (Fig. 1).

Small-Animal PET of Monkey Brain

Small-animal PET of ^{18}F -AV-45 in the monkey brain was evaluated after an intravenous injection (173.9 MBq [4.7 mCi]). The brain uptake kinetics (cortex and white matter) are presented in Figure 7. After an intravenous injection, ^{18}F -AV-45 penetrated the intact blood–brain barrier efficiently, and the activity in the cortex peaked at 7 min. The white matter region displayed a good uptake initially, but the activity washed out quickly. At 20 min after injection, the radioactivity in the cortex and white matter regions was similar. It is estimated that at the peak there was about 4.4% of the injected dose localized in the brain. This value reflected the fact that ^{18}F -AV-45 readily enters the monkey brain. Because there were no A β plaques in the healthy monkey brain, as expected, ^{18}F -AV-45 did not display any specific binding or prolonged retention in the brain.

DISCUSSION

AD is a progressive and often fatal disease. Symptoms include loss of memory (dementia) and other cognitive functions essential for maintaining normal daily activities (35,36). In addition, patients may show psychiatric symptoms and behavioral disturbances. Presently, autopsy and postmortem histologic analysis of the AD patient's brain samples is required for a definite diagnosis of the disease. Two major abnormal observations in the histopathologic examination of AD brain tissues are the hallmarks of this disease (37,38). The first is the presence of plaques, predominantly in the cortex and between neurons, produced by excess A β -amyloid protein aggregates. The second is the presence of tangles, inside neurons, composed of hyperphosphorylated τ -protein (1,37). It is generally accepted that PET for in vivo determination of these pathologic features will be useful for diagnostic purposes.

In addition to being a disease-defining pathologic marker of AD, A β plaques are believed to play a significant role in the pathophysiologic mechanisms of the disease. Accordingly, various strategies to prevent or reduce the accumulation of A β -amyloid protein aggregates—plaque burden—are now being pursued for the development of therapeutics for AD (39). Thus, PET agents, such as ^{18}F -AV-45, not only would assist the diagnosis of patients with AD but also may play a critical role in the development of antiplaque drugs by selecting those patients who have A β plaques in the brain and may benefit from drug treatment (40).

One of the essential prerequisites for a successful imaging agent for A β plaques in the brain is the ability to penetrate the intact blood–brain barrier. ^{18}F -AV-45 is a small and moderately lipophilic tracer, and it exhibits an excellent initial brain uptake in mice. Biodistribution studies in mice also show that the tracer not only has a high initial brain uptake but also displays fast washout kinetics from the healthy brain. These are highly desirable properties for a useful brain imaging agent targeting A β plaques. The favorable brain penetration and fast washout from healthy brain tissue were also demonstrated in healthy monkeys by small-animal PET (Fig. 7). An attractive combination of a high binding affinity to the A β plaque and fast

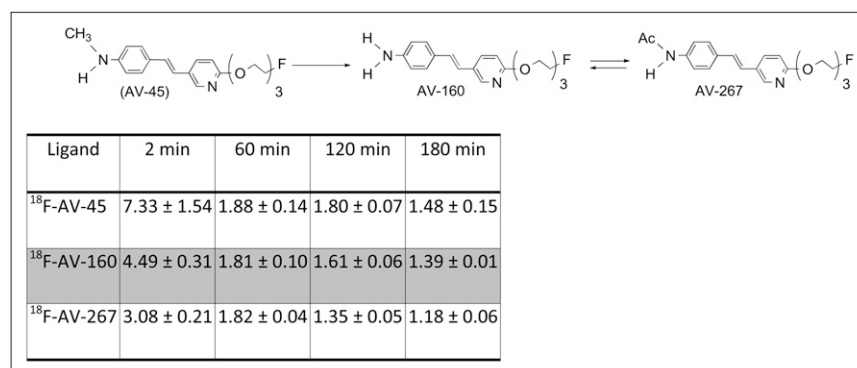


FIGURE 6. Brain uptakes and wash-out in healthy mice after injection of ^{18}F -AV-45 and its in vivo metabolites (% ID/g).

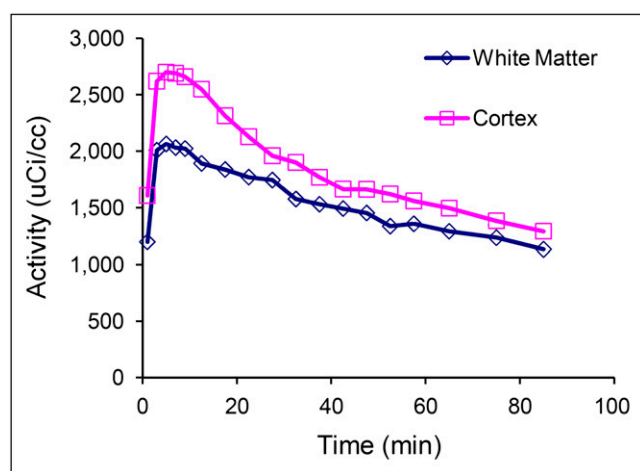


FIGURE 7. Kinetics of brain uptake and washout in rhesus monkey after intravenous injection of ^{18}F -AV-45 (173.9 MBq [4.7 mCi]) are presented. It is evident that uptake in cortex peaked at 7 min, and activity was washed out quickly thereafter. White matter area also displayed good initial uptake, and washout rate was also rapid. It is estimated that brain uptake at peak was about 4.4% of injected dose, which suggested that ^{18}F -AV-45 penetrated normal blood-brain barrier efficiently.

kinetics for washout from the healthy brain makes this agent decidedly successful in providing specific PET signals. Many reported A β plaque-targeting ligands, despite their high binding affinities, do not penetrate the brain, or once they enter the brain the nonspecific binding is so high that the agents cannot provide a specific signal for A β plaques. When ^{18}F -AV-45 was injected into transgenic mice in which abundant A β plaques were specially encoded in the brain, there was significant labeling of the A β plaques by this tracer (Fig. 5). The results further confirm that ^{18}F -AV-45 selectively binds to the A β plaques in the living brain.

Several metabolites of ^{18}F -AV-45 were identified in the blood of healthy mice (Fig. 6), and these metabolites were prepared and tested in healthy mice. They showed good brain uptake and a rapid washout with low nonspecific binding to the healthy brain. It is likely that the small amount of metabolites of ^{18}F -AV-45 in the blood will not affect binding of ^{18}F -AV-45 to A β plaques in vivo; furthermore, the metabolites themselves did not show specific binding to the A β plaques by in vitro binding assays. Contribution from these metabolites of ^{18}F -AV-45 during PET of the brain may be small.

^{18}F -AV-45 has several unique characteristics that make it suitable for A β plaque imaging in the living human brain: excellent binding affinity, as demonstrated by in vitro binding studies using AD brain homogenates; high selective A β plaque labeling, as demonstrated by in vitro autoradiography studies using postmortem AD brain sections; and excellent brain penetration and rapid kinetics in healthy mice and nonhuman primates (data not shown). As a further advantage, the radiochemistry of ^{18}F -AV-45 uses

a nucleophilic ^{18}F -fluoride substitution reaction and de-blocking of an *N*-protecting group, which is a relatively simple procedure. These features make it likely that manufacturing sites or radiopharmacies, which currently have established procedures for distributing clinical doses of ^{18}F -FDG for nuclear medicine clinics, can readily produce and distribute ^{18}F -AV-45.

One of major focal points of developing A β plaque imaging in the living human brain is the quantitative correlation of plaque density with the specific binding signal measured by PET. Currently, there are three ^{18}F -labeled A β plaque-specific PET agents, BAY 94-9172, GE-067, and ^{18}F -AV-45, under active commercial development. Human studies are now under way for ^{18}F -AV-45 with the goal of correlating PET with postmortem brain amyloid plaque pathology, the gold standard for demonstrating the A β plaque density in the brain.

CONCLUSION

The biodistribution studies of ^{18}F -AV-45 showed excellent brain uptake and washout kinetics in mice and monkey. Results of in vitro binding of postmortem AD brain tissue show an excellent binding profile for detecting A β plaques in the brain. The findings support the view that this PET agent may provide a convenient tool to investigate the presence of A β plaques in the brain of living human subjects.

ACKNOWLEDGMENTS

We thank Dr. Alan Carpenter for his helpful discussion and review of this manuscript. This work was supported by grants awarded from the National Institutes of Health (ROI-AG-022559 and R43AG032206).

REFERENCES

- Roberson ED, Mucke L. 100 years and counting: prospects for defeating Alzheimer's disease. *Science*. 2006;314:781–784.
- Hardy J. Has the amyloid cascade hypothesis for Alzheimer's disease been proved? *Curr Alzheimer Res*. 2006;3:71–73.
- Henneman WJ, Sluiter JD, Barnes J, et al. Hippocampal atrophy rates in Alzheimer disease: added value over whole brain volume measures. *Neurology*. 2009;72:999–1007.
- Minoshima S. Imaging Alzheimer's disease: clinical applications. *Neuroimaging Clin N Am*. 2003;13:769–780.
- Silverman DH. Brain ^{18}F -FDG PET in the diagnosis of neurodegenerative dementias: comparison with perfusion SPECT and with clinical evaluations lacking nuclear imaging. *J Nucl Med*. 2004;45:594–607.
- Barrio JR, Satyamurthy N, Huang SC, Petric A, Small GW, Kepe V. Dissecting molecular mechanisms in the living brain of dementia patients. *Acc Chem Res*. 2009;42:842–50.
- Small GW, Kepe V, Ercoli LM, et al. PET of brain amyloid and tau in mild cognitive impairment. *N Engl J Med*. 2006;355:2652–2663.
- Henriksen G, Yousefi BH, Drzezga A, Wester HJ. Development and evaluation of compounds for imaging of β -amyloid plaque by means of positron emission tomography. *Eur J Nucl Med Mol Imaging*. 2008;35(suppl 1):S75–S81.
- Cai L, Innis RB, Pike VW. Radioligand development for PET imaging of β -amyloid (A β): current status. *Curr Med Chem*. 2007;14:19–52.
- Mathis CA, Wang Y, Holt DP, Huang G-F, Debnath ML, Klunk WE. Synthesis and evaluation of ^{11}C -labeled 6-substituted 2-arylbenzothiazoles as amyloid imaging agents. *J Med Chem*. 2003;46:2740–2754.
- Klunk WE, Engler H, Nordberg A, et al. Imaging brain amyloid in Alzheimer's disease with Pittsburgh compound-B. *Ann Neurol*. 2004;55:306–319.

12. Mathis CA, Klunk WE, Price JC, DeKosky ST. Imaging technology for neurodegenerative diseases: progress toward detection of specific pathologies. *Arch Neurol*. 2005;62:196–200.
13. Klunk WE, Mathis CA. The future of amyloid- β imaging: a tale of radionuclides and tracer proliferation. *Curr Opin Neurol*. 2008;21:683–687.
14. Svedberg MM, Hall H, Hellstrom-Lindahl E, et al. [^{11}C]PIB-amyloid binding and levels of A β 40 and A β 42 in postmortem brain tissue from Alzheimer patients. *Neurochem Int*. 2008;54:347–357.
15. Tolboom N, Yaqub M, van der Flier WM, et al. Detection of Alzheimer pathology in vivo using both ^{11}C -PIB and ^{18}F -FDDNP PET. *J Nucl Med*. 2009;50:191–197.
16. Engler H, Santillo AF, Wang SX, et al. In vivo amyloid imaging with PET in frontotemporal dementia. *Eur J Nucl Med Mol Imaging*. 2008;35:100–106.
17. Mathis CA, Ikonomicb MD, Debnath ML, Hamilton RL, DeKosky ST, Klunk WE. Comparison of the binding of 3'-F-PiB and PiB in human brain homogenates. *Neuroimage*. 2008;41(suppl 2):T113–T114.
18. Kung MP, Zhuang ZP, Hou C, Kung HF. Development and evaluation of iodinated tracers targeting amyloid plaques for SPECT imaging. *J Mol Neurosci*. 2004;24:49–53.
19. Kung MP, Hou C, Zhuang Z-P, et al. IMPY: an improved thioflavin-T derivative for in vivo labeling of β -amyloid plaques. *Brain Res*. 2002;956:202–210.
20. Newberg AB, Wintering NA, Plossl K, et al. Safety, biodistribution, and dosimetry of ^{123}I -IMPY: a novel amyloid plaque-imaging agent for the diagnosis of Alzheimer's disease. *J Nucl Med*. 2006;47:748–754.
21. Newberg AB, Wintering NA, Clark CM, et al. Use of ^{123}I IMPY SPECT to differentiate Alzheimer's disease from controls [abstract]. *J Nucl Med*. 2006; 47(suppl 1):78P.
22. Lin KS, Debnath ML, Mathis CA, Klunk WE. Synthesis and β -amyloid binding properties of rhenium 2-phenylbenzothiazoles. *Bioorg Med Chem Lett*. 2009; 19:2258–2262.
23. Maya Y, Ono M, Watanabe H, Haratake M, Saji H, Nakayama M. Novel radioiodinated aurones as probes for SPECT imaging of beta-amyloid plaques in the brain. *Bioconjug Chem*. 2009;20:95–101.
24. Kung HF, Lee C-W, Zhuang ZP, Kung MP, Hou C, Plossl K. Novel stilbenes as probes for amyloid plaques. *J Am Chem Soc*. 2001;123:12740–12741.
25. Qu W, Kung MP, Hou C, Benedum TE, Kung HF. Novel styrylpyridines as probes for SPECT imaging of amyloid plaques. *J Med Chem*. 2007;50:2157–2165.
26. Zhang W, Oya S, Kung MP, Hou C, Maier DL, Kung HF. F-18 stilbenes as PET imaging agents for detecting β -amyloid plaques in the brain. *J Med Chem*. 2005;48:5980–5988.
27. Zhang W, Kung MP, Oya S, Hou C, Kung HF. ^{18}F -labeled styrylpyridines as PET agents for amyloid plaque imaging. *Nucl Med Biol*. 2007;34:89–97.
28. Ono M, Haratake M, Nakayama M, et al. Synthesis and biological evaluation of (E)-3-styrylpyridine derivatives as amyloid imaging agents for Alzheimer's disease. *Nucl Med Biol*. 2005;32:329–335.
29. Zhang W, Oya S, Kung MP, Hou C, Maier DL, Kung HF. F-18 PEG stilbenes as PET imaging agents targeting A β aggregates in the brain. *Nucl Med Biol*. 2005;32:799–809.
30. Ono M, Wilson A, Nobrega J, et al. ^{11}C -labeled stilbene derivatives as A β -aggregate-specific PET imaging agents for Alzheimer's disease. *Nucl Med Biol*. 2003;30:565–571.
31. Verhoeff NP, Wilson AA, Takeshita S, et al. In vivo imaging of Alzheimer disease beta-amyloid with [^{11}C]SB-13 PET. *Am J Geriatr Psychiatry*. 2004; 12:584–595.
32. Stephenson KA, Chandra R, Zhuang ZP, et al. Fluoro-pegylated (FPEG): imaging agents targeting A β aggregates. *Bioconjug Chem*. 2007;18:238–246.
33. Rowe CC, Ackerman U, Browne W, et al. Imaging of amyloid β in Alzheimer's disease with ^{18}F -BAY94-9172, a novel PET tracer: proof of mechanism. *Lancet Neurol*. 2008;7:129–135.
34. Kung M-P, Hou C, Zhuang Z-P, Cross AJ, Maier DL, Kung HF. Characterization of IMPY as a potential imaging agent for β -amyloid plaques in double transgenic PSAPP mice. *Eur J Nucl Med Mol Imaging*. 2004;31:1136–1145.
35. Burns A, Iliffe S. Alzheimer's disease. *BMJ*. 2009;338:b158.
36. Burns A, Iliffe S. Dementia. *BMJ*. 2009;338:b75.
37. Erten-Lyons D, Woltjer RL, Dodge H, et al. Factors associated with resistance to dementia despite high Alzheimer disease pathology. *Neurology*. 2009;72: 354–360.
38. Braak H, Braak E. Diagnostic criteria for neuropathologic assessment of Alzheimer's disease. *Neurobiol Aging*. 1997;18(suppl):S85–S88.
39. Rafii MS, Aisen PS. Recent developments in Alzheimer's disease therapeutics. *BMC Med*. 2009;7:7.
40. Mathis CA, Lopresti BJ, Klunk WE. Impact of amyloid imaging on drug development in Alzheimer's disease. *Nucl Med Biol*. 2007;34:809–822.



The Journal of
NUCLEAR MEDICINE

Preclinical Properties of ^{18}F -AV-45: A PET Agent for A β Plaques in the Brain

Seok Rye Choi, Geoff Golding, Zhiping Zhuang, Wei Zhang, Nathaniel Lim, Franz Hefti, Tyler E. Benedum, Michael R. Kilbourn, Daniel Skovronsky and Hank F. Kung

J Nucl Med. 2009;50:1887-1894.

Published online: October 16, 2009.

Doi: 10.2967/jnumed.109.065284

This article and updated information are available at:
<http://jnm.snmjournals.org/content/50/11/1887>

Information about reproducing figures, tables, or other portions of this article can be found online at:
<http://jnm.snmjournals.org/site/misc/permission.xhtml>

Information about subscriptions to JNM can be found at:
<http://jnm.snmjournals.org/site/subscriptions/online.xhtml>

The Journal of Nuclear Medicine is published monthly.
SNMMI | Society of Nuclear Medicine and Molecular Imaging
1850 Samuel Morse Drive, Reston, VA 20190.
(Print ISSN: 0161-5505, Online ISSN: 2159-662X)

© Copyright 2009 SNMMI; all rights reserved.

The logo for the Society of Nuclear Medicine and Molecular Imaging (SNMMI) consists of the letters 'S', 'N', 'M', and 'I' arranged in a 2x2 grid. Each letter is white and set within a red square. To the right of this grid, the full name of the society is written in a smaller, black, sans-serif font.
SOCIETY OF
NUCLEAR MEDICINE
AND MOLECULAR IMAGING